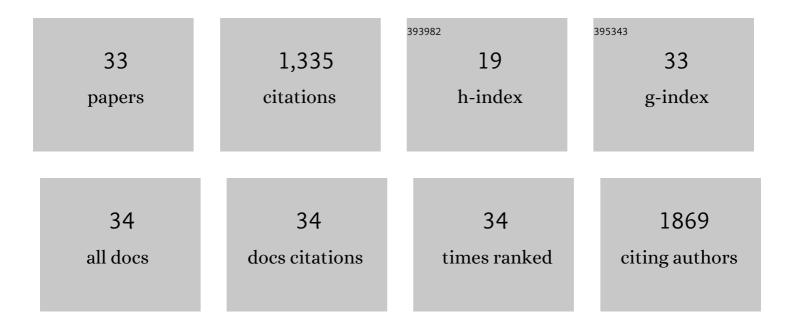
## De-Bo Hu

List of Publications by Year in descending order

Source: https://exaly.com/author-pdf/2122814/publications.pdf Version: 2024-02-01



DF-Ro Hu

#	Article	IF	CITATIONS
1	Active control of micrometer plasmon propagation in suspended graphene. Nature Communications, 2022, 13, 1465.	5.8	31
2	Tunable Planar Focusing Based on Hyperbolic Phonon Polaritons in αâ€MoO <sub>3</sub> . Advanced Materials, 2022, 34, e2105590.	11.1	32
3	Few-layer hexagonal boron nitride as a shield of brittle materials for cryogenic s-SNOM exploration of phonon polaritons. Applied Physics Letters, 2022, 120, .	1.5	2
4	Ultrasensitive Midâ€Infrared Biosensing in Aqueous Solutions with Graphene Plasmons. Advanced Materials, 2022, 34, e2110525.	11.1	20
5	Ghost hyperbolic surface polaritons in bulk anisotropic crystals. Nature, 2021, 596, 362-366.	13.7	102
6	Antifouling hydrogel film based on a sandwich array for salivary glucose monitoring. RSC Advances, 2021, 11, 27561-27569.	1.7	10
7	Low-fouling CNT-PEG-hydrogel coated quartz crystal microbalance sensor for saliva glucose detection. RSC Advances, 2021, 11, 22556-22564.	1.7	9
8	Nanoimaging and Nanospectroscopy of Polaritons with Time Resolved <i>s</i> NOM. Advanced Optical Materials, 2020, 8, 1901042.	3.6	22
9	Probing Polaritons in 2D Materials. Advanced Optical Materials, 2020, 8, 1901416.	3.6	13
10	The development of an antifouling interpenetrating polymer network hydrogel film for salivary glucose monitoring. Nanoscale, 2020, 12, 22787-22797.	2.8	10
11	Ultrasensitive Poly(boric acid) Hydrogel-Coated Quartz Crystal Microbalance Sensor by Using UV Pressing-Assisted Polymerization for Saliva Glucose Monitoring. ACS Applied Materials & Interfaces, 2020, 12, 34190-34197.	4.0	26
12	Hybrid hydrogel films with graphene oxide for continuous saliva-level monitoring. Journal of Materials Chemistry C, 2020, 8, 9655-9662.	2.7	8
13	Efficient Allâ€Optical Plasmonic Modulators with Atomically Thin Van Der Waals Heterostructures. Advanced Materials, 2020, 32, e1907105.	11.1	44
14	Structural colouration in the Himalayan monal, hydrophobicity and refractive index modulated sensing. Nanoscale, 2020, 12, 21409-21419.	2.8	6
15	A Multibeam Interference Model for Analyzing Complex Nearâ€Field Images of Polaritons in 2D van der Waals Microstructures. Advanced Functional Materials, 2019, 29, 1904662.	7.8	10
16	High-efficiency modulation of coupling between different polaritons in an in-plane graphene/hexagonal boron nitride heterostructure. Nanoscale, 2019, 11, 2703-2709.	2.8	24
17	Tunable Modal Birefringence in a Low‣oss Van Der Waals Waveguide. Advanced Materials, 2019, 31, e1807788.	11.1	27
18	Modern Scatteringâ€Type Scanning Nearâ€Field Optical Microscopy for Advanced Material Research. Advanced Materials, 2019, 31, e1804774.	11.1	205

De-Bo Hu

#	Article	IF	CITATIONS
19	30 s Response Time of K <sup>+</sup> Ionâ€Selective Hydrogels Functionalized with 18â€Crownâ€6 Ether Based on QCM Sensor. Advanced Healthcare Materials, 2018, 7, 1700873.	3.9	15
20	Flexible and Electrically Tunable Plasmons in Graphene–Mica Heterostructures. Advanced Science, 2018, 5, 1800175.	5.6	38
21	Largeâ€Scale Suspended Graphene Used as a Transparent Substrate for Infrared Spectroscopy. Small, 2017, 13, 1603812.	5.2	13
22	High performance boronic acid-containing hydrogel for biocompatible continuous glucose monitoring. RSC Advances, 2017, 7, 41384-41390.	1.7	24
23	Probing optical anisotropy of nanometer-thin van der waals microcrystals by near-field imaging. Nature Communications, 2017, 8, 1471.	5.8	74
24	Study of graphene plasmons in graphene–MoS <sub>2</sub> heterostructures for optoelectronic integrated devices. Nanoscale, 2017, 9, 208-215.	2.8	36
25	Farâ€Field Spectroscopy and Nearâ€Field Optical Imaging of Coupled Plasmon–Phonon Polaritons in 2D van der Waals Heterostructures. Advanced Materials, 2016, 28, 2931-2938.	11.1	77
26	Far-field nanoscale infrared spectroscopy of vibrational fingerprints of molecules with graphene plasmons. Nature Communications, 2016, 7, 12334.	5.8	237
27	Broadly tunable graphene plasmons using an ion-gel top gate with low control voltage. Nanoscale, 2015, 7, 19493-19500.	2.8	90
28	Resonant Mirror Enhanced Raman Spectroscopy. Journal of Physical Chemistry C, 2014, 118, 13099-13106.	1.5	7
29	Refractive-Index-Enhanced Raman Spectroscopy and Absorptiometry of Ultrathin Film Overlaid on an Optical Waveguide. Journal of Physical Chemistry C, 2013, 117, 16175-16181.	1.5	19
30	Eigenmodes in a negative-refractive-index planar waveguide for high-sensitivity evanescent sensing and spectroscopic applications. Proceedings of SPIE, 2013, , .	0.8	1
31	Microdisplacement Sensor Based on Tilted Fiber Bragg Grating Transversal Load Effect. IEEE Sensors Journal, 2011, 11, 1776-1779.	2.4	23
32	Simultaneous measurement of liquid level and surrounding refractive index using tilted fiber Bragg grating. Sensors and Actuators A: Physical, 2011, 170, 62-65.	2.0	53
33	Hydraulic pressure sensor based on fiber Bragg grating. Optical Engineering, 2011, 50, 064401.	0.5	26